

Minigaps in strained silicon quantum wells on tilted substrates

T. J. Thornton,^{a)} F. Ge, A. Andresen, D. Pivin, J. Bird, and D. K. Ferry
*Department of Electrical Engineering and Center for Solid State Electronics Research,
Arizona State University, Tempe, Arizona 85287-5706*

(Received 19 January 1999; accepted 3 May 1999)

The two-dimensional electron gas formed at the inverted surface of a tilted silicon substrate shows unusual magnetotransport properties due to the presence of a minigap in the density of states. For metal-oxide-semiconductor inversion layers the strong scattering at the interface limits the mobility to values $\mu < 10\text{--}20\,000\text{ cm}^2/\text{V s}$. To achieve mobilities approaching $10^5\text{ cm}^2/\text{V s}$ we have used strained Si:SiGe quantum wells grown on substrates tilted away from the (001) normal by 0° , 2° , 4° , 6° , and 10° . Their transport properties have been measured in the temperature range of 20–500 mK. All the samples show strong Shubnikov-de Haas oscillations. For the 2° and 4° samples the envelope of the fast oscillations is modulated by a longer period oscillation at low magnetic fields. We attribute the slow oscillation in the 2° and 4° samples to the presence of a minigap. For the 6° and 10° samples the minigap is higher than the Fermi energy and is not expected to influence the transport properties. © 1999 American Vacuum Society.
[S0734-211X(99)05604-8]

I. INTRODUCTION

Tilted substrates have been used to explore a number of issues related to semiconductor interfaces. Vicinal GaAs substrates, i.e., those tilted a few degrees from high symmetry planes such as the (001) and (111) have been used to study the growth of quantum wires¹ and lateral surface superlattices^{2,3} and for investigating dopant incorporation.⁴ Vicinal silicon substrates have an even longer history, having been used in the early years of metal-oxide-semiconductor (MOS) technology to find Si:SiO₂ interfaces with the lowest interface state density.⁵ Silicon wafers with high index surfaces such as (11 n) are readily available and correspond to offcut angles of a few degrees between the surface normal and the [001] direction. Surprisingly, silicon MOS inversion layers on (115) and (118) substrates have shown curious transport anomalies,^{6,7} which were later explained by the formation of a minigap in the density of states.⁸ Recently, Si:SiGe quantum wells on tilted substrates have been used to reduce the density of threading dislocations⁹ present in these strained layers as well as to explore the nucleation of dislocations¹⁰ via the modified Frank-Read mechanism. Strained silicon quantum wells on tilted substrates also show interesting surface morphology as well as anisotropic transport properties.^{11,12} In this article we describe recent transport measurements of modulation doped Si:SiGe quantum wells on various offcut substrates at temperatures down to 20 mK. The results are consistent with the formation of a minigap in the density of states. We begin with a discussion of the layer structure and surface morphology of these layers.

II. LAYER STRUCTURE AND SURFACE MORPHOLOGY

The strained silicon quantum wells used in this work all had similar layer structures (see Fig. 1) and were grown

by gas source molecular beam epitaxy (MBE), the details of which have been presented elsewhere.¹³ Approximately 1% tensile strain is required in the silicon channel to produce the necessary conduction band offset. This can be achieved by growing a thin silicon layer on a relaxed SiGe substrate with a germanium concentration in the range of 20%–30%. In our case the germanium concentration in the buffer layer is increased linearly from 0% to 29% over a thickness of $2\text{ }\mu\text{m}$ and is followed by $1\text{ }\mu\text{m}$ of Si_{0.72}Ge_{0.28}. The $100\text{ }\text{Å}$ thick quantum well is modulation doped, i.e., it is separated from $500\text{ }\text{Å}$ of heavily doped Si_{0.72}Ge_{0.28} by a $150\text{ }\text{Å}$ spacer layer with the same alloy concentration. The layers are capped with $50\text{ }\text{Å}$ of silicon.

During growth of the graded buffer layer, threading dislocations nucleate and are free to glide on the four equivalent {111} planes producing strain relieving misfit segments (60° dislocations). Surface steps due to the 60° misfit dislocations¹⁴ and reduced growth rates near to them¹⁵ lead to the well known “cross-hatch” pattern on the sample surface. The {111} glide planes intersect the surface of standard (001) substrates along $\langle 110 \rangle$ directions and the cross hatching is orthogonal. However, on tilted substrates such as (11 n) the situation is different.^{11,12} Two of the {111} planes still intersect the surface along $[\bar{1}10]$. The other two planes align at a small angle $\alpha/2$ on either side of [110], given by

$$\cos \alpha = \frac{2 \cos^2 \phi + \sin^2 \phi}{2 \cos^2 \phi + 3 \sin^2 \phi}, \quad (1)$$

where $\phi = \arccos(n/\sqrt{n^2+1})$ is the offcut angle between the surface normal and the [001]. The different surface morphologies for an on-axis and a 6° off-axis sample are shown in Fig. 2 and measurements of α for different values of ϕ confirm the relationship in Eq. (1).¹²

The surface roughness of the cross hatching shown in Fig. 2 has a typical correlation length of 5–10 μm with a root mean square (rms) amplitude of $\sim 10\text{ nm}$ for the on-axis

^{a)}Electronic mail: t.thornton@asu.edu

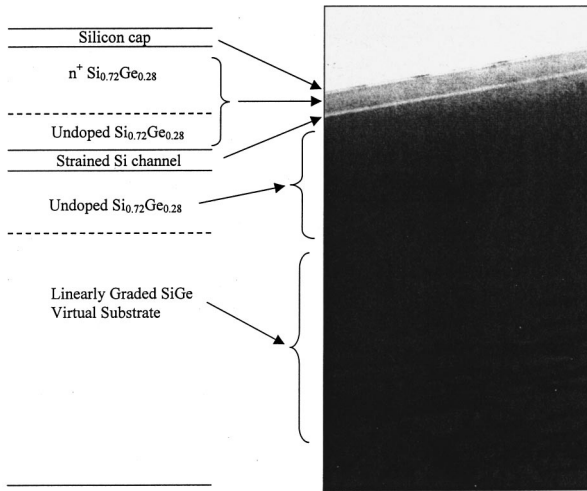


FIG. 1. Layer structure and cross-sectional transmission electron microscopy (TEM) micrograph of one of the strained silicon quantum wells. All of the samples used had similar layer structures. The TEM cross section confirms that the dislocations are buried below the quantum well.

sample, decreasing to ~ 5 nm for the higher off-cut angle samples. Despite the fact that the surface roughness is comparable to the thickness of the quantum well it does not seem to unduly influence the electron mobility, with values as high as $95\,000\text{ cm}^2/\text{Vs}$ being obtained for the quantum wells grown on (001) substrates. However, as the tilt angle is increased, additional surface features with a much smaller length scale develop due to the formation of terraces on the (11*n*) surface. In Fig. 3 an atomic force microscopy (AFM) image of the 6° sample shows the terraces running along the $[\bar{1}10]$ direction. The surface of Si(11*n*) substrates consists of single and double steps¹⁶ and assuming an even mixture the average terrace height and width can be calculated. For a 6° off-cut substrate the average terrace width would be ~ 2 nm. In fact, the average terrace width and height in Fig. 3 is 17 and 2 nm, respectively, suggesting that considerable step bunching has occurred.

III. ELECTRON TRANSPORT ON TILTED SUBSTRATES

The presence of the terraces leads to anisotropic transport properties for the quantum wells grown on tilted substrates.^{11,12} For transport perpendicular to the step edges

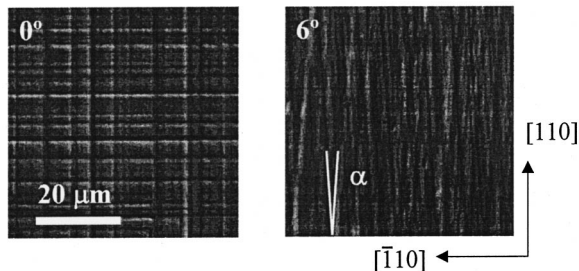


FIG. 2. Nomarski optical micrographs of the surface of the on-axis and 6° tilted samples.

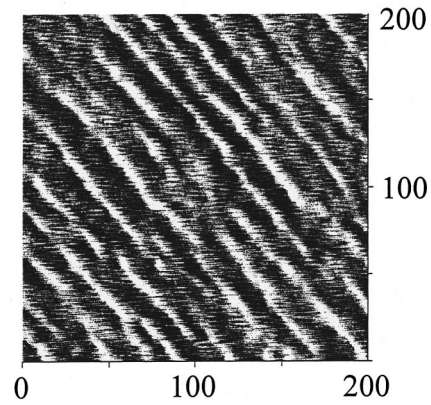


FIG. 3. $200\text{ nm} \times 200\text{ nm}$ AFM image of the surface of the 6° sample. The terraces are parallel to the $[110]$ direction.

extra electron scattering reduces the mobility compared to values measured parallel to the terraces. Figure 4 shows the sheet resistance as a function of magnetic field for a 10° off-cut sample at a temperature of 0.4 K. The samples have standard Hall bar geometries aligned parallel and perpendicular to the step edges. the Shubnikov–de Haas (SdH) oscillations arise from Landau quantization of the density of states as a result of the large magnetic field. They have the same periodicity in each case confirming that the measured sheet density is the same. The higher resistance measured with a current flowing perpendicular to the terraces confirms the lower mobility of this orientation. The mobility measurements are summarized in Table I. The results show a general trend towards increasing anisotropy in the mobility for increasing off-cut angle.

When cooled to lower temperatures the amplitude of the SdH oscillations increases as expected from the reduction in thermal broadening. The 2° and 4° samples, however, show an additional slow oscillation at low fields. The amplitude of the new oscillation is small and easily obscured by the background magnetoresistance and the much larger amplitude of the fast oscillations. In Fig. 5 we show the low field SdH

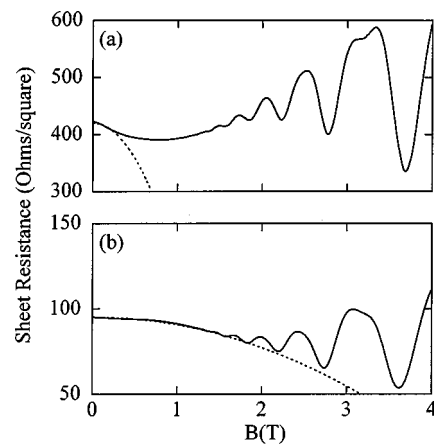


FIG. 4. Magnetoresistance of the 10° sample measured (a) perpendicular and (b) parallel to the terrace edges. The measurement temperatures were (a) 400 and (b) 600 mK.

TABLE I. Electron mobilities and sheet densities of the samples used in this work.

Off-cut angle (deg)	Electron mobility ($\text{cm}^2/\text{V s}$)		Sheet density (10^{11} cm^{-2})
	μ_{\parallel}	μ_{\perp}	
0	95 000	95 000	6.9
2	69 400	69 800	9.7
4	45 200	35 300	7.4
6	43 300	40 000	7.1
10	62 600	14 200	10.5

oscillations of the 0° , 2° , 4° , and 6° samples after subtraction of a quadratic term describing the background magnetoresistance.¹⁷ For a uniform two-dimensional electron gas (2DEG) with a sheet density N_s the oscillations have a periodicity that is given by $\Delta(1/B) = 4e/N_s\hbar$ and another of twice the frequency if the field is large enough that the spin splitting can be resolved. The data in Fig. 5 are plotted against inverse magnetic field to highlight the $1/B$ periodicity. The slow oscillation is weaker in the 2° sample than in the 4° sample and is not present at all in the 6° , 10° , and on-axis samples. The Fourier transforms of the data from the 0° , 2° , and 4° samples plotted against sheet density are shown in Fig. 6. All of the fast Fourier transform (FFT) spectra have a distinct peak corresponding to sheet densities of 6.9 , 9.7 , and $7.4 \times 10^{11} \text{ cm}^{-2}$ for the 0° , 2° , and 4° samples, respectively. However, only the 2° and 4° samples have a distinct peak at frequencies corresponding to lower electron concentrations. This additional peak is due to the slow oscillation present in the data of Figs. 5(b) and 5(c).

Results similar to those in Figs. 5 and 6 have been reported for silicon MOS inversion layers on 1.2° and 10° off-cut substrates.^{6,18} In both these cases a slow oscillation evolved into a faster oscillation with increasing magnetic

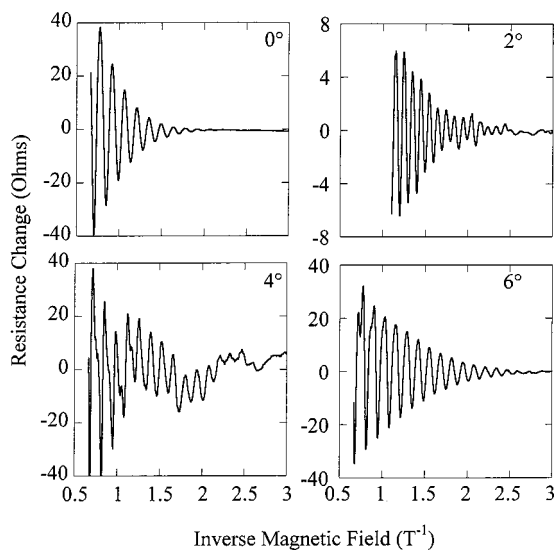


FIG. 5. Magnetoresistance of the 0° , 2° , 4° , and 6° samples plotted against inverse magnetic field. The measurement temperature for the on-axis sample was 80 mK and was less than 20 mK for the others. The background magnetoresistance was subtracted from the data.

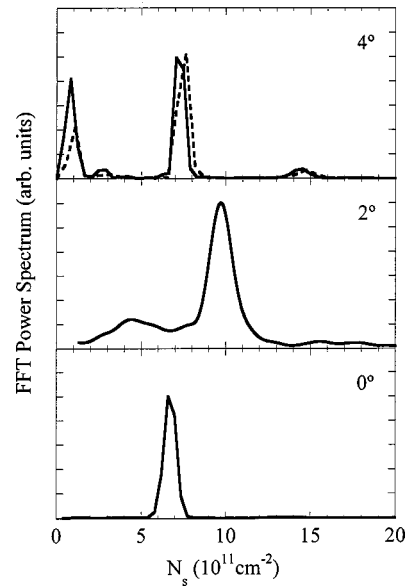


FIG. 6. FFT power spectra for the 0° , 2° , and 4° data of Fig. 5 (solid lines). The dashed line shows the FFT from the 4° sample at a temperature of 400 mK.

field and the results were interpreted in terms of the so-called valley projection model (VPM) which predicts the existence of a minigap in the density of states.⁸ For a 2DEG on a (001) substrate there are two low energy valleys in the E - k dispersion with minima at $(0, 0, \pm k_0)$ where $k_0 = 0.85(2\pi/a)$, a being the lattice constant, which is 5.43 \AA for silicon. When projected onto the (001) surface the two valleys are coincident and the valley degeneracy is 2. However, when projected onto a low angle vicinal substrate such as $(11n)$ the valleys no longer coincide but cross at points given by $k = 0.15k_0 \sin \varphi$ where φ is the off-cut angle. The degeneracy is lifted at the crossing points due to valley-valley interactions and a minigap is formed. The width of the minigap increases with the sheet density and off-cut angle and is typically⁸ a few meV for densities of a few 10^{12} cm^{-2} .

Figure 7 illustrates the occupation of the conduction band in the 2° , 4° , and 6° samples and can be used to explain the results of Fig. 5. For both the 2° and 4° samples the minigap is located below the Fermi energy, E_F . The lower band is completely full and for small magnetic fields only the upper band contributes to the SdH oscillations with a periodicity corresponding to a sheet density N_{slow} , i.e., the slow oscillations observed in the 2° and 4° samples. As the magnetic field increases, tunneling can occur through the minigap and for fields such that $E_g = \hbar\omega_c$ magnetic breakdown¹⁹ occurs and the minigap cannot be resolved. At this point the SdH oscillations are faster with a periodicity corresponding to a sheet density N_{fast} . The situation for the 4° sample is similar except now the minigap is higher in energy, because of the larger tilt angle, and the Fermi energy in this sample is smaller. For the 6° sample the minigap is higher than the Fermi energy and only the faster oscillations are observed. Although this argument explains the qualitative behavior we observe, the position of the minigap is not in quantitative

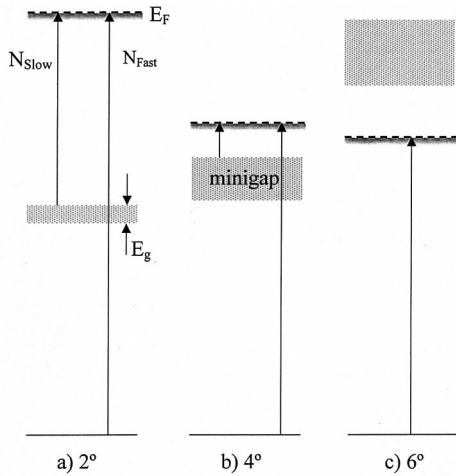


FIG. 7. Schematic illustration of the electron occupancy in the conduction band for the 2°, 4°, and 6° samples. The vertical arrows represent the carriers contributing to the fast and slow oscillations observed in the magnetoresistance.

agreement. For vicinal MOS field effect transistors (MOSFETs) the lowest minigap would occur at an energy corresponding to a sheet density of 1.2 and $4.7 \times 10^{11} \text{ cm}^{-2}$ for the 2° and 4° samples, respectively. The values of N_{fast} and N_{slow} that we obtain would place the energy gap at an occupancy of approximately 4 and $6 \times 10^{11} \text{ cm}^{-2}$ although, without knowing the exact width of the minigaps in each case, assigning accurate values is difficult.

We have measured the low field SdH oscillations in the 4° sample as a function of temperature in an attempt to determine the width of the minigaps. The amplitude of the slow oscillation peak in the FFT power spectrum decreases with temperature as is shown in Fig. 6. By extrapolation to zero amplitude the slow oscillation component vanishes at a temperature of $\sim 0.75 \text{ K}$ corresponding to a thermal energy of $65 \mu\text{eV}$. If thermal broadening were reducing the width of the minigap and consequently reducing the amplitude of the slow SdH component, then $65 \mu\text{eV}$ would be a lower estimate for the width of the minigap. However, this value is smaller than we expect from comparison with vicinal MOSFETs, and thermal broadening may be reducing the amplitude via other mechanisms.

The minigap can also be estimated from the magnetic field at which breakdown occurs, i.e., when the fast oscillations first appear. For the 4° sample this value is approximately 0.4 T and assuming $E_g = \hbar \omega_c$ we get an energy gap of 0.24 meV. Again, this value is somewhat smaller than we would expect from a similar MOSFET sample but the additional strain in the silicon quantum well may be influencing the width of the minigap.

IV. CONCLUSION

We have measured the transport properties of strained silicon quantum wells on substrates tilted away from the (001) normal by 0°, 2°, 4°, 6°, and 10°. All the layers shows cross hatching with a characteristic length scale of $10 \mu\text{m}$ while the tilted substrates show terracing with much smaller characteristic length scales. The extra scattering induced by the terraces leads to anisotropic electron mobility when measured parallel and perpendicular to the step edges. At the lowest temperatures an additional slow oscillation is seen in the magnetoresistance of the 2° and 4° samples that we attribute to the presence of a minigap.

ACKNOWLEDGMENT

The authors thank Dr. Juan Fernandez of Imperial College, London, for growing the strained silicon samples used in this work.

- ¹B. A. Joyce, J. H. Neave, J. Zhang, D. D. Vvedensky, S. Clakre, K. J. Hugill, T. Shitara, and A. K. Myersbeaghton, *Semicond. Sci. Technol.* **5**, 1147 (1990).
- ²M. S. Miller, H. Weman, C. E. Pryor, M. Krishnamurthy, P. M. Petroff, H. Kroemer, and J. L. Merz, *Phys. Rev. Lett.* **68**, 3464 (1992).
- ³T. Fukui, K. Tsubaki, H. Saito, M. Kasu, and S. Honda, *Surf. Sci.* **267**, 588 (1992).
- ⁴M. R. Fahy, J. H. Neave, M. J. Ashwin, R. Murray, R. C. Newman, B. A. Joyce, Y. Kadoya, and H. Sakaki, *J. Cryst. Growth* **127**, 871 (1993).
- ⁵H. Sakaki (private communication).
- ⁶P. J. Stiles, T. Cole, and A. A. Lakhani, *J. Vac. Sci. Technol.* **14**, 969 (1997).
- ⁷T. Cole, A. A. Lakhani, and P. J. Stiles, *Phys. Rev. Lett.* **38**, 722 (1997).
- ⁸L. J. Sham, S. J. Allen, A. Kamgar, and D. C. Tsui, *Phys. Rev. Lett.* **40**, 472 (1978).
- ⁹G. L. Zhou, Z. Ma, M. E. Lin, L. H. Allen, and H. Markoç, *Appl. Phys. Lett.* **63**, 2094 (1993).
- ¹⁰P. M. Mooney, F. K. LeGoues, J. Tersoff, and J. O. Chu, *J. Appl. Phys.* **75**, 3968 (1994).
- ¹¹T. J. Thornton, J. M. Fernandez, S. Kaya, P. W. Green, and K. Fobelets, *Appl. Phys. Lett.* **70**, 1278 (1997).
- ¹²P. Waltereit, J. M. Fernandez, S. Kaya, and T. J. Thornton, *Appl. Phys. Lett.* **72**, 2262 (1998).
- ¹³J. M. Fernandez, A. Matsumura, X. M. Zhang, M. H. Xie, L. Hart, T. J. Thornton, and B. A. Joyce, *J. Mater. Sci.* **6**, 330 (1995).
- ¹⁴S. Y. Shirayev, F. Jensen, and J. W. Peterson, *Appl. Phys. Lett.* **64**, 3305 (1994).
- ¹⁵E. A. Fitzgerald, Y. H. Xie, D. Monroe, P. J. Silverman, J. M. Kuo, A. R. Kortan, F. A. Thiel, and B. E. Weir, *J. Vac. Sci. Technol. B* **10**, 1807 (1992).
- ¹⁶J. Wasserful and W. Ranke, *Surf. Sci.* **315**, 227 (1994).
- ¹⁷T. J. Thornton, A. Matsumura, and J. Fernandez, *Surf. Sci.* **361/362**, 547 (1996).
- ¹⁸S. M. Goodnick, J. R. Sites, K. S. Yi, D. K. Ferry, and C. W. Wilmsen, *Phys. Lett.* **97A**, 111 (1983).
- ¹⁹A. B. Pippard, *Proc. R. Soc. London, Ser. A* **207**, 1 (1962).